BELTCON 8

24, 25 & 26 October 1995

THE TWO-DIMENSIONAL DYNAMIC BEHAVIOUR OF CONVEYOR BELTS

AUTHOR : IR GABRIËL LODEWIJKS

DELFT UNIVERSITY OF
TECHNOLOGY
MEKELWEG 2
2628 CD DELFT
THE NETHERLANDS

TELEPHONE : *0931 15 78 3827*
FACSIMILE : *0931 15 78 1397*

The Two-Dimensional Dynamic Behaviour of Conveyor Belts

Ir. G. Lodewijks, Delft University of Technology, The Netherlands

1. SUMMARY

In this paper a new finite element model of a belt-conveyor system will be introduced. This model has been developed in order to be able to simulate both the longitudinal and transverse dynamic response of the belt during starting and stopping. Application of the model in the design stage of long overland belt-conveyor systems enables the engineer, for example, to design proper belt-conveyor curves by detecting premature lifting of the belt off the idlers. It also enables the design of optimal idler spacing and troughing configuration in order to ensure resonance-free belt motion by determining (standing) longitudinal and transverse belt vibrations. Application of feed-back control techniques enables the design of optimal starting and stopping procedures whereas an optimal belt can be selected by taking the dynamic properties of the belt into account.

2. INTRODUCTION

The Netherlands has long been recognised as a country in which transport and transhipment play a major role in the economy. The port of Rotterdam, in particular is known as the gateway to Europe and claims to have the largest harbour system in the world. Besides the large numbers of containers, a large volume of bulk goods also passes through this port. Not all these goods are intended for the Dutch market, many have other destinations and are transhipped in Rotterdam. Good examples of typical bulk goods that are transhipped are coal and iron ore, a significant part of which is intended for the German market. In order to handle the bulk materials a wide range of different mechanical conveyors including belt-conveyors is used.

The length of most belt-conveyor systems erected in the Netherlands is relatively small, since they are mainly used for in-plant movement of bulk materials. The longest belt-conveyor system, which is about 2 km long, is situated on the Maasvlakte, part of the port of Rotterdam, where it is used to transport coal from a bulk terminal to an electricity power station. In addition to domestic projects, an increasing number of Dutch engineering consultancies participates in international projects for the development of large overland belt-conveyor systems. This demands the understanding of typical difficulties encountered during the development of these systems, which are studied in the Department of Transport Technology of the Faculty of Mechanical Engineering, Delft University of Technology, one of the three Dutch Universities of Technology.

The interaction between the conveyor belt properties, the bulk solids properties, the belt conveyor configuration and the environment all influence the level to which the conveyor-system meets its predefined requirements. Some interactions cause troublesome phenomena so research is initiated into those phenomena which cause practical problems, [1]. One way to classify these problems is to divide them into the category which indicate their underlying causes in relation to the description of belt conveyors.

The two most important dynamic considerations in the description of belt conveyors are the reduction of transient stresses in non-stationary moving belts and the design of belt-conveyor lay-outs for resonance-free operation, [2]. In this paper a new finite element model of a belt-conveyor system will be presented which enables the simulation of the belt's longitudinal and transverse response to starting and stopping procedures and it's motion during steady state operation. It's beyond the scope of this paper to discuss the results of the simulation of a start-up procedure of a belt-conveyor system, therefore an example will be given which show some possibilities of the model.

3. FINITE ELEMENT MODELS OF BELT-CONVEYOR SYSTEMS

If the total power supply, needed to drive a belt-conveyor system, is calculated with design standards like DIN 22101 then the belt is assumed to be an inextensible body. This implies that the forces exerted on the belt during starting and stopping can be derived from Newtonian rigid body dynamics which yields the belt stress. With this belt stress the maximum extension of the belt can be calculated. This way of determining the elastic response of the belt is called the quasi-static (design) approach. For small belt-conveyor systems this leads to an acceptable design and acceptable operational behaviour of the belt. For long belt-conveyor systems, however, this may lead to a poor design, high maintenance costs, short conveyor-component life and well known operational problems like :

- excessive large displacement of the weight of the gravity take-up device
- premature collapse of the belt, mostly due to the failure of the splices
- destruction of the pulleys and major damage of the idlers
- lifting of the belt off the idlers which can result in spillage of bulk material
- damage and malfunctioning of (hydrokinetic) drive systems

Many researchers developed models in which the elastic response of the belt is taken into account in order to determine the phenomena responsible for these problems. In most models the belt-conveyor model consists of finite elements in order to account for the variations of the resistance's and forces exerted on the belt. The global elastic response of the belt is made up by the elastic response of all its elements. These finite element models have been applied in computer software which can be used in the design stage of (long) belt-conveyor systems. This is called the dynamic (design) approach. Verification of the results of simulation has shown that software programs based on these kind of belt-models are quite successful in predicting the elastic response of the belt during starting and stopping, see for example [3] and [4] .

The finite element models as mentioned above determine only the longitudinal elastic response of the belt. Therefore they fail in the accurate determination of:

- the motion of the belt over the idlers and the pulleys
- the dynamic drive phenomena
- the bending resistance of the belt
- the development of (shock) stress waves
- the interaction between the belt sag and the propagation of longitudinal stress waves
- the interaction between the idler and the belt
- the influence of the belt speed on the stability of motion of the belt
- the dynamic stresses in the belt during passage of the belt over a (driven) pulley
- the influence of parametric resonance of the belt due to the interaction between vibrations of the take up mass or eccentricities of the idlers and the transverse displacements of the belt
- the development of standing transverse waves
- the influence of the damping caused by bulk material and by the deformation of the cross-sectional area of the belt and bulk material during passage of an idler
- the lifting of the belt off the idlers in convex and concave curves

The transverse elastic response of the belt is often the cause of breakdowns in long belt-conveyor systems and should therefore be taken into account. The transverse response of a belt can be determined with special models as proposed in [5] and [6], but it is more convenient to extend the present finite element models with special elements which take this response into account.

3.1 THE BELT

A typical belt-conveyor geometry consisting of a drive pulley, a tail pulley, a vertical gravity take-up, a number of idlers and a plate support is shown in Figure 1. This geometry is taken as an example to illustrate how a finite element model of a belt conveyor can be developed when only the longitudinal elastic response of the belt is of interest.

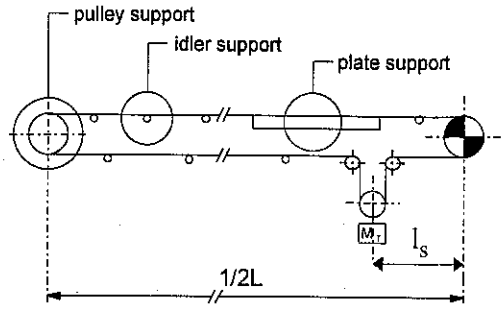

Figure 1: *Typical belt-conveyor geometry.*

Since the length of the belt part between the drive pulley and the take-up pulley, l_s, is negligible compared to the length of the total belt, L, these pulleys can mathematically be combined to one pulley as long as the mass inertia's of the pulleys of the take-up system are accounted for. Since the resistance forces encountered by the belt during motion vary from place to place depending on the exact local (maintenance) conditions and geometry of the belt conveyor, these forces are distributed along the length of the belt. In order to be able to determine the influence of these distributed forces on the motion of the belt, the belt is divided into a number of finite elements and the forces which act on that specific part of the belt are allocated to the corresponding element. If the interest is in the longitudinal elastic response of the belt only then the belt is not discretised on those places where it is supported by a pulley which does not force its motion (slip possible). This is shown in Figure 2. The last step in building the model is to replace the belt's drive and tensioning system by two forces which represent the drive characteristic and the tension forces. A more extended description of the process of building a finite element model of a belt conveyor can be found in [7].

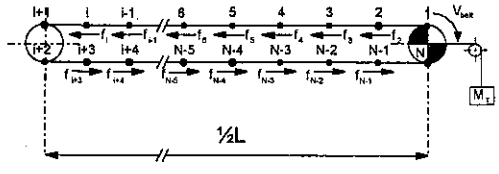

Figure 2: *Belt divided into finite elements.*

The exact interpretation of the finite elements depends on which resistance's and influences of the interaction between the belt and its supporting structure are taken into account and the mathematical description of the constitutive behaviour of the belt material. Depending on this interpretation, the elements can be represented

by a system of masses, springs and dashpots as is shown in Figure 3, [9], where such a system is given for one finite element with nodal points c and c+1. The springs K and dashpot H represent the visco-elastic behaviour of the belt's tensile member, G represents the belt's variable longitudinal geometric stiffness produced by the vertical acting forces on the belt's cross section between two idlers, C represents the transitional static to dynamic friction and V represent the belts velocity dependent resistance's.

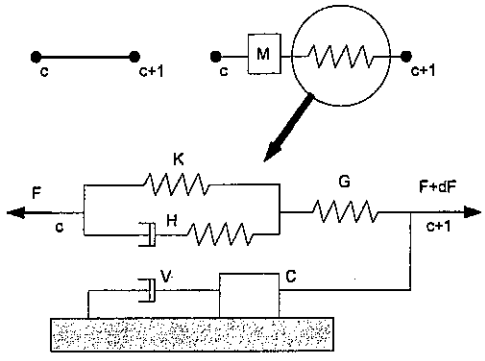

Figure 3: *Five element composite model [9].*

3.1.1 NON LINEAR TRUSS ELEMENT

If only the longitudinal deformation of the belt is of interest then a truss element can be used to model the elastic response of the belt. A truss element as shown in Figure 4 has two nodal points, p and q, and four displacement parameters which determine the component vector x:

$$x^T = \left[u_p \quad v_p \quad u_q \quad v_q\right] \qquad (1)$$

For the in-plane motion of the truss element there are three independent rigid body motions therefore one deformation parameter remains which describes

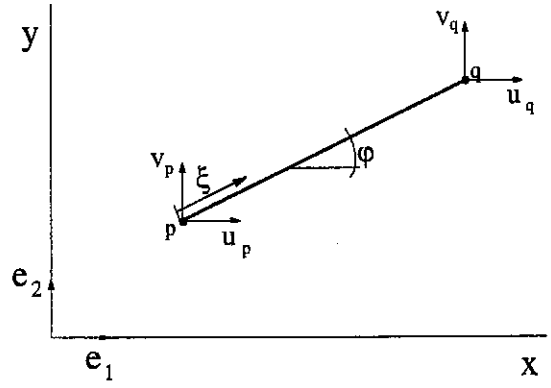

Figure 4: *Definition of the displacements of a truss element*

the change of length of the axis of the truss element [7]:

$$\varepsilon_l = \mathbf{D}_l(x) = \int_0^1 \frac{ds^2 - ds_0^2}{2ds_0^2} d\xi \qquad (2)$$

where ds_0 is the length of the undeformed element, ds the length of the deformed element and ξ a dimensionless length coordinate along the axis of the element.

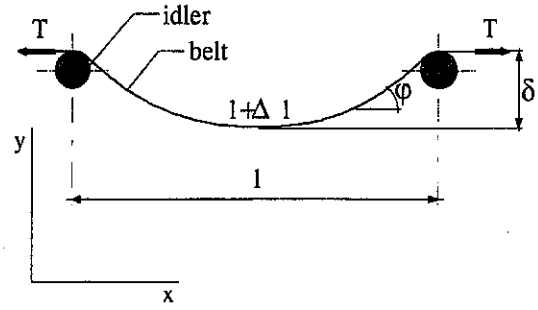

Figure 5: *Static sag of a tensioned belt*

Although bending deformations are not included in the truss element, it is possible to take the static influence of small values of the belt sag into account. The static belt sag ratio is defined by (see Figure 5):

$$K_s = \frac{\delta}{l} = \frac{ql}{8T} \qquad (3)$$

where q is the distributed vertical load exerted on the belt by the weight of the belt and the bulk material, l the idler space and T the belt tension. The effect of the belt sag on the longitudinal deformation is determined by [7]:

$$\varepsilon_s = \frac{8}{3} K_s^2 \qquad (4)$$

which yields the total longitudinal deformation of the non linear truss element:

$$\varepsilon_l^* = \mathbf{D}_l^*(x) = \varepsilon_l + \varepsilon_s \qquad (5)$$

3.1.2 BEAM ELEMENT

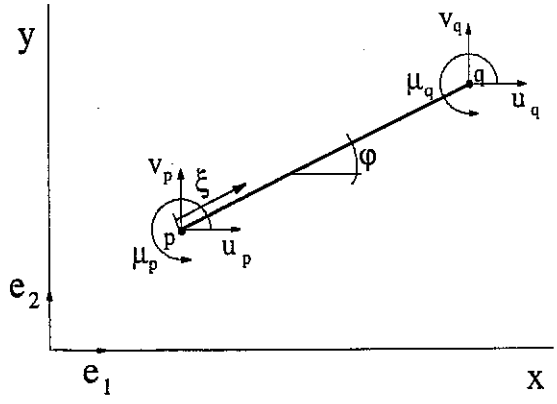

Figure 6: *Definition of the nodal point displace-ments and rotations of a beam element.*

If the transverse displacement of the belt is being of interest then the belt can be modelled by a beam element. Also for the in-plane motion of a beam element, which has six displacement parameters, there are three independent rigid body motions. Therefore three deformation parameters remain: the longitudinal deformation parameter, ε_1, and two bending deformation parameters, ε_2 and ε_3.

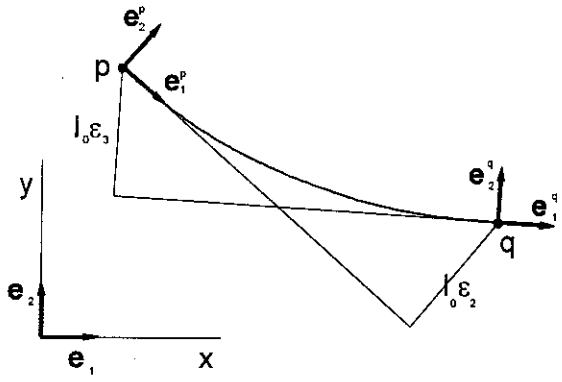

Figure 7: *The bending deformations of a beam element.*

The bending deformation parameters of the beam element can be defined with the component vector of the beam element (see Figure 6):

$$x^T = \left[u_p \quad v_p \quad \mu_p \quad u_q \quad v_q \quad \mu_q\right] \qquad (6)$$

and the deformed configuration as shown in Figure 7:

$$\varepsilon_2 = \mathbf{D}_2(x) = \frac{\mathbf{e}_2^p \mathbf{l}_{pq}}{l_0}$$
$$\varepsilon_3 = \mathbf{D}_3(x) = \frac{-\mathbf{e}_2^q \mathbf{l}_{pq}}{l_0} \qquad (7)$$

3.2 THE MOVEMENT OF THE BELT OVER IDLERS AND PULLEYS

The movement of a belt is constrained when it moves over an idler or a pulley. In order to account for these constraints, constraint (boundary) conditions have to be added to the finite element description of the belt. This can be done by using multi-body dynamics. The classic description of the dynamics of multi-body mechanisms is developed for rigid bodies or rigid links which are connected by several constraint conditions. In a finite element description of a (deformable) conveyor belt, where the belt is discretised in a number of finite elements, the links between the elements are deformable. The finite elements are connected by nodal points and therefore share displacement parameters. To determine the movement of the belt, the rigid body modes are eliminated from the deformation modes. If a belt moves over an idler then the length coordinate ξ, which determines the position of the belt on the idler, see Figure 8, is added to the component vector, eq. (6), thus resulting in a vector of seven displacement parameters.

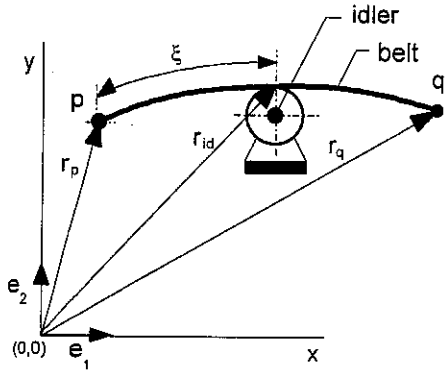

Figure 8: *Belt supported by an idler.*

There are two independent rigid body motions for an in-plane supported beam element therefore five deformation parameters remain. Three of them, ε_1, ε_2 and ε_3 , determine the deformation of the belt and are already given in 3.1. The remaining two, ε_4 and ε_5, determine the interaction between the belt and the idler, see Figure 9.

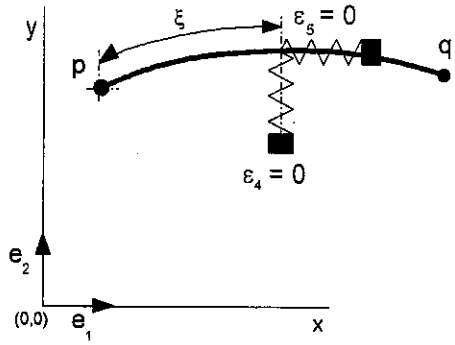

Figure 9: *FEM beam element with two constraint conditions.*

These deformation parameters can be imagined as springs of infinite stiffness. This implies that:

$$\varepsilon_4 = \mathbf{D}_4(x) = \left(\mathbf{r}_\xi + \mathbf{u}_\xi\right)\mathbf{e}_2 - \mathbf{r}_{id}.\mathbf{e}_2 = 0$$
$$\varepsilon_5 = \mathbf{D}_5(x) = \left(\mathbf{r}_\xi + \mathbf{u}_\xi\right)\mathbf{e}_1 - \mathbf{r}_{id}.\mathbf{e}_1 = 0 \qquad (8)$$

If during simulation $\varepsilon_4 > 0$ then the belt is lifted off the idler and the constraint conditions are removed from the finite element description of the belt.

3.3 THE ROLLING RESISTANCE

In order to enable application of a model for the rolling resistance in the finite element model of the belt conveyor an approximate formulation for this resistance has been developed, [8]. Components of the total rolling resistance which is exerted on a belt

during motion three parts that account for the major part of the dissipated energy, can be distinguished including: the indentation rolling resistance, the inertia of the idlers (acceleration rolling resistance) and the resistance of the bearings to rotation (bearing resistance). Parameters which determine the rolling resistance factor include the diameter and material of the idlers, belt parameters such as speed, width, material, tension, the ambient temperature, lateral belt load, the idler spacing and trough angle. The total rolling resistance factor that expresses the ratio between the total rolling resistance and the vertical belt load can be defined by:

$$f_t = f_i + f_a + f_b \tag{9}$$

where f_i is the indentation rolling resistance factor, f_a the acceleration resistance factor and f_b the bearings resistance factor. These components are defined by:

$$f_i = C F_z^{n_z} h^{n_h} D^{-n_D} V_b^{n_v} K_N^{-n_k} T^{n_T}$$

$$f_a = \frac{m_{red}}{F_z b} \frac{\partial^2 u}{\partial t^2} \tag{10}$$

$$f_b = \frac{M_f}{F_z b r_i}$$

where F_z is distributed vertical belt and bulk material load, h the thickness of the belt cover, D the idler diameter, V_b the belt speed, K_N the nominal percent belt load, T the ambient temperature, m_{red} the reduced mass of an idler, b the belt width, u the longitudinal displacement of the belt, M_f the total bearing resistance moment and r_i the internal bearing radius. The dynamic and mechanic properties of the belt and belt cover material play an important role in the calculation of the rolling resistance. This enables the selection of belt and belt cover material which minimise the energy dissipated by the rolling resistance.

3.4 THE BELT'S DRIVE SYSTEM

To enable the determination of the influence of the rotation of the components of the drive system of a belt conveyor, as shown in Figure 10, on the stability of motion of the belt, a model of the drive system is included in the total model of the belt conveyor. The transition elements of the drive system, as for example the reduction box, are modelled with constraint conditions as described in section 3.2. A reduction box with reduction ratio i can be modelled by a reductionbox element with two displacement parameters, μ_p and μ_q, one rigid body motion (rotation) and therefore one deformation parameter :

$$\varepsilon_{red} = \mathbf{D}_{red}(x) = i\mu_p + \mu_q = 0 \tag{11}$$

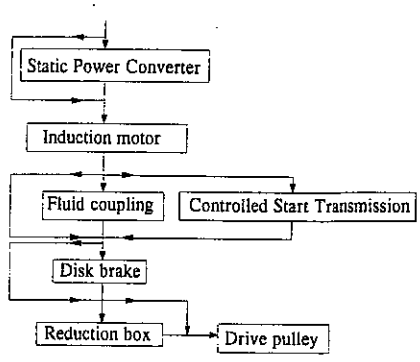

Figure 10: *Possible components of the drive system of belt conveyors.*

To determine the electrical torque of an induction machine, the so-called two axis representation of an electrical machine is adapted, see Figure 11, [7]. The vector of phase voltages **v** can be obtained from:

$$\mathbf{v} = \mathbf{R}\mathbf{i} + \omega_s \mathbf{G}\mathbf{i} + \mathbf{L}\frac{\partial \mathbf{i}}{\partial t} \tag{12}$$

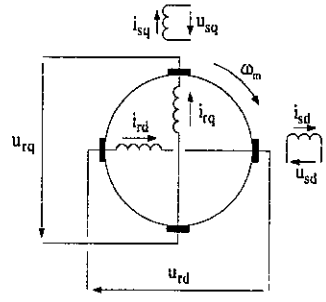

Figure 11: *Two axis representation of induction motor in stator coordinates.*

In eq. (11) **i** is the vector of phase currents, **R** the matrix of phase resistance's, **G** the matrix of inductive phase resistance's, **L** the matrix of phase inductance's and ω_s the electrical angular velocity of the rotor. The electro-magnetic torque is equal to:

$$T_e = \mathbf{i}^T \mathbf{G} \mathbf{i} \tag{13}$$

The connection of the motor model and the mechanical components of the drive system is given by the equations of motion of the drive system:

$$\mathbf{T}_i = \mathbf{I}_{ij} \frac{\partial^2 \varphi_j}{\partial t^2} + \mathbf{C}_{ik} \frac{\partial \varphi_k}{\partial t} + \mathbf{K}_{il} \varphi_l \tag{14}$$

where **T** is the torque vector, **I** the inertia matrix, **C** the damping matrix, **K** the stiffness matrix and φ the angle of rotation of the drive component axis's.

To simulate a controlled start or stop procedure a feedback routine can be added to the

model of the belt's drive system in order to control the drive torque.

3.5 THE EQUATIONS OF MOTION

The equations of motion of the total belt conveyor model can be derived with the principle of virtual power which leads to [7]:

$$f_k - M_{kl}\frac{\partial^2 x_l}{\partial t^2} = \sigma_i D_{ik} \qquad (15)$$

where **f** is the vector of resistance forces, **M** the mass matrix and σ the vector of multipliers of Lagrange which may be interpret as the vector of stresses dual to the vector of strains ε. To arrive at the solution for **x** from this set of equations, integration is necessary. However the results of the integration have to satisfy the constraint conditions. If the zero prescribed strain components of for example eq. (8) have a residual value then the results of the integration have to be corrected, also see [7]. It is possible to use the feed-back option of the model for example to restrict the vertical movement of the take-up mass. This inverse dynamic problem can be formulated as follows. Given the model of the belt and its drive system, the motion of the take-up system known, determine the motion of the remaining elements in terms of the degrees of freedom of the system and its rates. It is beyond the scope of this paper to discuss all the details of this option.

3.6 EXAMPLE

Application of the FEM in the design stage of long belt conveyor systems enables its proper design. The selected belt strength, for example, can be minimised by minimising the maximum belt tension using the simulation results of the model. As an example of the features of the finite element model, the transverse vibration of a span of a stationary moving belt between two idler stations will be considered. This should be determined in the design stage of the conveyor in order to ensure resonance free belt support.

The effect of the interaction between idlers and a moving belt is important in belt-conveyor design. Geometric imperfections of idlers and pulleys cause the belt on top of these supports to be displaced, yielding a transverse vibration of the belt between the supports. This imposes an alternating axial stress component in the belt. If this component is small compared to the pre-stress of the belt then the belt will vibrate in it's natural frequency, otherwise the belt's vibration will follow the imposed excitation. The belt can for example be excitated by an eccentricity of the idlers. This kind of vibrations is particularly noticeable on belt conveyor returns. Since the frequency of the imposed excitation depends on the angular speed of the pulleys and idlers, and thus on the belt speed, it is important to determine the influence of the belt speed on the natural frequency of the transverse vibration of the belt between two supports. If the frequency of the imposed excitation approaches the natural frequency of transverse vibration of the belt, resonance phenomena occur.

The results of simulation with the finite element model can be used to determine the frequency of transverse vibration of a stationary moving belt span. This frequency is obtained after transformation of the results of the transverse displacement of the belt span from the time domain to the frequency domain using the fast fourier technique. Besides using the finite element model also an analytical approach can be used.

The belt can be modelled as a pre-stressed beam. If the bending stiffness of the belt is neglected, the transverse displacements are small compared to the idler space, $K_s \ll 1$, and the increase of the belt length due to the transverse displacement is negligible compared to its initial length, the transverse vibration of the belt can be approximated by the following linear differential equation, also see Figure 5:

$$\frac{\partial^2 v}{\partial t^2} = \left(c_2^2 - V_b^2\right)\frac{\partial^2 v}{\partial x^2} - 2V_b\frac{\partial^2 v}{\partial x \partial t} \qquad (16)$$

where v is the transverse displacement of the belt and c_2 the wave speed of the transverse waves defined by, [1]:

$$c_2 = \sqrt{\frac{gl}{8K_s}} \qquad (17)$$

The first natural transverse frequency of the belt span of Figure 5 can be obtained from eq. (16) if it is assumed that v(0,t)=v(l,t)=0 :

$$f_b = \frac{1}{2l}c_2\left(1-\beta^2\right) \qquad (18)$$

where β is the dimensionless speed ratio defined by:

$$\beta = \frac{V_b}{c_2} \qquad (19)$$

The frequency f_b is different for each individual belt span since the belt tension varies over the length of the conveyor. The excitation frequency of an idler which has a single eccentricity is equal to:

$$f_i = \frac{V_b}{\pi D} \qquad (20)$$

where D is the diameter of the idler. In order to design a resonance free belt support the idler space is subjected to the following condition:

$$L \neq \frac{\pi D}{2\beta}\left(1-\beta^2\right) \qquad (21)$$

The results obtained with the linear differential equation (16) however are valid only for low values of the ratio β. For higher values of β, as is the case for high-speed conveyors or low belt tensions, the non-linear terms in the full form of eq. (16) become significant. Therefore numerical simulations using the FEM model have been made in order to determine the ratio between the linear (eq. 18) and the non-linear frequency of transverse vibration of a belt span . These relations have been determined for different values of β as a function of the sag ratio K_s. After numerical simulation a result as shown in Figure 12 was obtained.

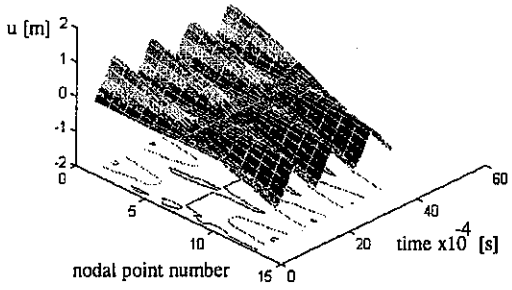

Figure 12: *Longitudinal displacements of nodal points of a finite element model of a conveyor belt.*

The results for the transverse displacements were transformed to a frequency spectrum using a fast-fourier technique. The frequencies obtained from these spectra were compared to the frequencies obtained from eq. (18) which yielded the curves as shown in Figure 13. From this figure it follows that for β smaller that 0.3 the calculation errors are small. For higher values of β the calculation error made by a linear approximation is more than 10 %. Application of a finite element model of the belt which uses non-linear beam elements therefore enables an accurate determination of the transverse vibrations for high values of β.

For lower values of β the frequencies of transverse vibration can also be predicted accurate by eq. (18). However it is not possible to analyse, for example, the interaction between the belt sag and the propagation of longitudinal waves or the lifting of the belt off the idlers as can be done with the finite element model.

The determined relation between the belt stress and the frequency of transverse vibrations can also be used in belt tension monitoring systems.

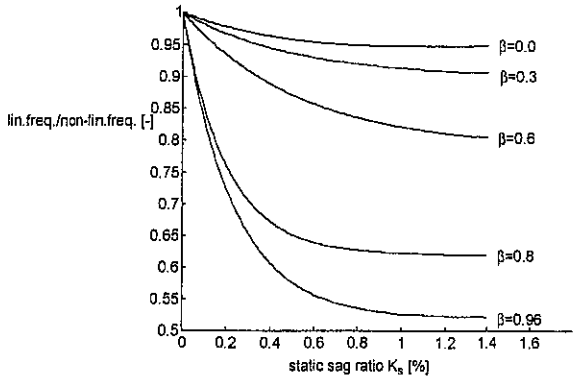

Figure 13: *Ratio between the linear and the non-linear frequency of transverse vibration of a belt span supported by two idlers.*

4. EXPERIMENTAL VERIFICATION

In order to be able to verificate the results of the simulations, experiments have been carried out with the dynamic test facility shown in Figure 14.

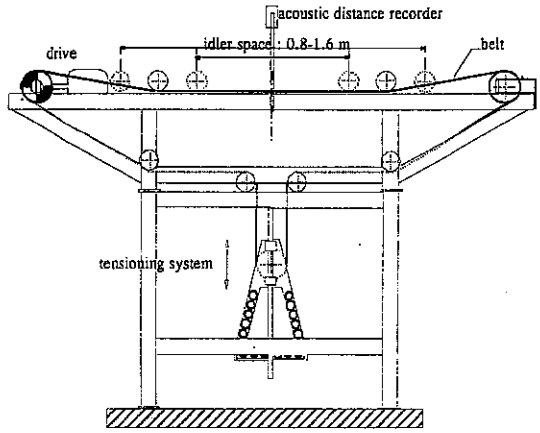

Figure 14: *Dynamic test facility.*

With this test facility the transverse vibration of an unloaded flat belt span between two idlers, as for example a return part, can be determined. An acoustic device is used to measure the displacement of the belt. Besides that, also the tensioning force, belt speed, motor torque, idler rotations and idler space were known during the experiments. Some results of the experiments are shown in the Figures 15 and 16. Figure 15 shows the relation between the natural frequency of transverse vibration of a belt span and the belt speed as measured during the experiments, calculated by eq. (18), with and without speed dependency, thus neglecting the term β in eq. (18), and obtained from the numerical simulations. In the Figures 16 the frequencies are given as a function of β instead of V_b to enable comparison with the results shown in Figure 13. Figure 16a and b show the errors made by the calculations as compared to the result of the experiments. Also from these figures it can be

learned that for β above 0.3 the linear approximations are no longer accurate.

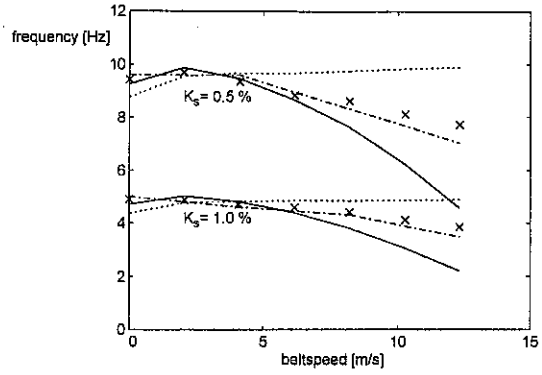

Figure 15: *Measured (cross marks) and calculated frequencies of transverse vibration of a supported belt part. (linear speed independent model (dotted line), linear speed dependent model (solid line) and non-linear model (dash-dot line))*

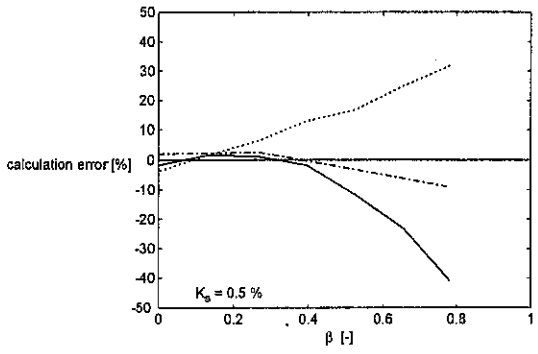

Figure 16a: *Calculation errors made by calculation of the frequencies of transverse vibration of a supported belt part with the linear speed independent model (dotted line), linear speed dependent model (solid line) and non-linear model (dash-dot line) for K_s=0.5 %.*

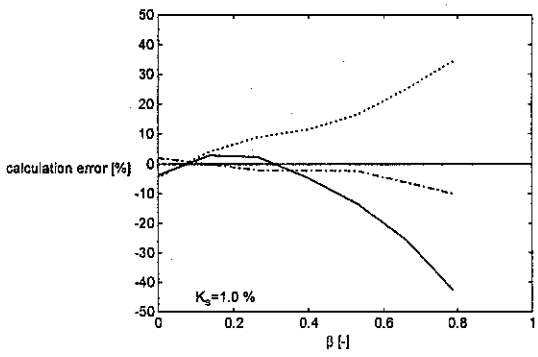

Figure 16b: *Calculation errors made by calculation of the frequencies of transverse vibration of a supported belt part with the linear speed independent model (dotted line), linear speed dependent model (solid line) and non-linear model (dash-dot line) for K_s=1.0 %.*

5. EXAMPLE

Since the most cost-effective operation conditions of belt conveyors occur in the range of belt widths 0.6 - 1.2 m ,[2], the belt's capacity can be varied by varying the belt speed. However before the belt speed is varied the interaction between the belt and the idler should be determined in order to ensure resonance free belt support. To illustrate this the transverse displacement of a stationary moving belt span between two idlers have been measured. The total belt length L was 52.7 m, the idler space l was 3.66 m, the static sag ratio K_s 2.1 %, β was 0.24 and the belt speed V_b 3.57 m/s. Figure 17 shows the ratio between the transverse displacement and the static belt sag as a function of time.

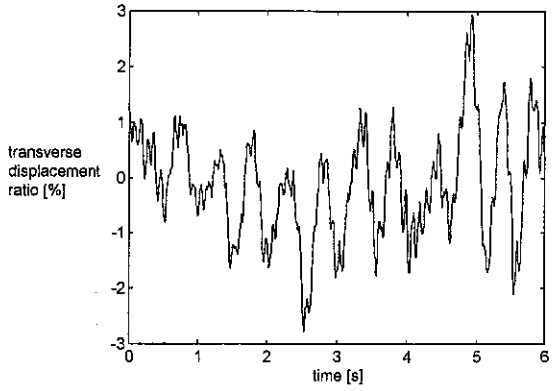

Figure 17: *Transverse vibration of a stationary moving belt span supported by two idlers.*

After transformation of this signal by a fast fourier technique the frequency spectrum of Figure 18 was obtained. In Figure 18 three frequencies appear. The first frequency is caused by the passage of the belt splice:

$$f_s = \frac{V_b}{L} = 0.067\,\text{Hz} \qquad (22)$$

The second frequency, which appears at 1.94 Hz, is caused by the transverse vibration of the belt .

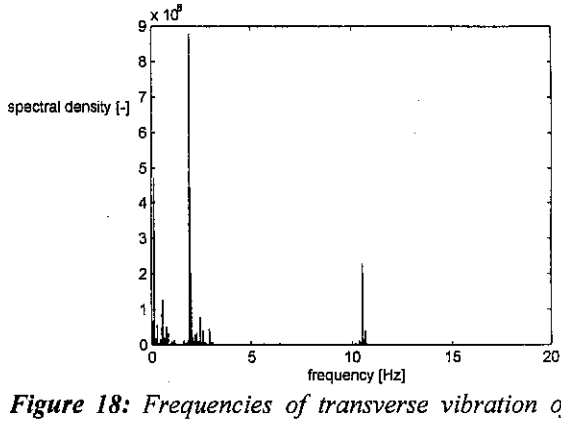

Figure 18: *Frequencies of transverse vibration of a stationary moving belt span supported by two idlers.*

The third frequency which appears at 10.5 Hz is caused by the rotation of the idlers. From the numerical simulations Figure 19 was obtained.

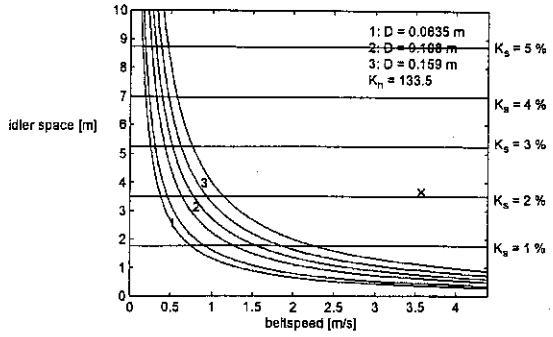

Figure 19: *Calculated resonance zone's for different idler diameters D. Cross indicates belt speed and idler space during experiment.*

Figure 19 shows the zone's where resonance caused by the belt/idler interaction may be expected for three idler diameters. The idlers of the belt conveyor had a diameter of 0.108 m thus resonance phenomena may be expected nearby a belt speed of 0.64 m/s. To check this, the maximum transverse displacement of the belt span has been measured during a start-up of the conveyor.

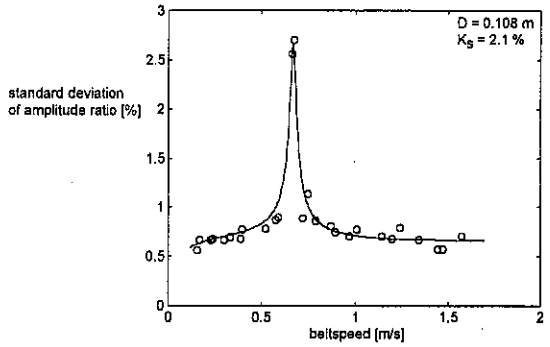

Figure 20: *Measured ratio of the standard deviation of the amplitude of transverse vibration and the static belt sag .*

As can be seen in Figure 20 the maximum amplitude of the transverse vibration occur at a belt speed of 0.64 m/s as was predicted by the results of simulation with the finite element model. Therefore the belt speed should not be chosen nearby 0.64 m/s. Although a flat belt is used for the experiments and the theoretical verification, the applied techniques can also be used for troughed belts.

6. CONCLUSIONS

Application of beam elements in finite element models of belt conveyors enable the simulation of the transverse displacement of the belt thus enabling the design of resonance free belt supports. The advantage of applying beam elements for small values of β instead of using a linear differential equation to predict resonance phenomena is that also the interaction between the longitudinal and transverse displacement of the belt and the lifting of the belt off the idlers can be predicted from simulation.

7. REFERENCES

1. Lodewijks, G. (1995), "Present Research at Delft University of Technology, The Netherlands", 1995 5th International Conference on Bulk Material Storage, Handling and Transportation, Newcastle, Australia, 10-12 July 1995, The Institution of Engineers, Australia Preprints pp. 381-394.
2. Roberts, A.W. (1994), "Advances in the design of Mechanical Conveyors", Bulk Solids Handling **14**, pp. 255-281.
3. Nordell, L.K. and Ciozda, Z.P. (1984), "Transient belt stresses during starting and stopping: Elastic response simulated by finite element methods", Bulk Solids Handling **4**, pp. 99-104.
4. Funke, A. and Könneker, F.K. (1988), "Experimental investigations and theory for the design of a long-distance belt-conveyor system", Bulk Solids Handling **8**, pp. 567-579.
5. Harrison, A. (1984), "Flexural behaviour of tensioned conveyor belts", Bulk Solids Handling **4**, pp. 67-71.
6. Lodewijks, G. (1994), "Transverse vibrations in flexible belt systems", Delft University of Technology, report no. 94.3.TT.4270.
7. Lodewijks, G. (1994), "On the Application of Beam Elements in Finite Element Models of Belt Conveyors, Part I", Bulk Solids Handling **14**, pp. 729-737.
8. Lodewijks, G. (1995), "The Rolling Resistance of Belt Conveyors", Bulk Solids Handling **15**, pp. 15-22.
9. Nordell, L.K. and Ciozda, Z.P. (1984), "Transient belt stresses during starting and stopping: Elastic response simulated by finite element methods", Bulk Solid Handling **11**, pp. 99-104.